

Fluctuation effects in superconducting nanostrips

A. Engel^{a,b,1} A.D. Semenov^b H.-W. Hübers^b K. Il'in^c
M. Siegel^c

^a*Physics Institute of the University of Zurich, Winterthurerstr. 190, 8057 Zurich, Switzerland*

^b*DLR Institute of Planetary Research, Rutherfordstr. 2, 12489 Berlin, Germany*

^c*Institute of Micro- and Nano-Electronic Systems, University of Karlsruhe, Hertzstr. 16, 76187 Karlsruhe, Germany*

Abstract

Superconducting fluctuations in long and narrow strips made from ultrathin NbN films, have been investigated. For large bias currents close to the critical current fluctuations led to localized, temporary transitions into the normal conducting state, which were detected as voltage transients developing between the strip ends. We present models based on fluctuations in the Cooper pair density and current-assisted thermal-unbinding of vortex-antivortex pairs, which explain the current and temperature dependence of the experimental fluctuation rates.

Key words: low-dimensional superconducting structures, fluctuations, vortices
PACS: 74.40.+k, 74.78.-w, 85.25.-j

1 Introduction

One of the key properties of superconductors, zero resistance, has always been in the focus with regard to possible applications of superconducting materials. The outcome of these efforts can be seen in the wide-spread use of MRI-scanners and their superconducting magnets in hospitals, for example. Not least due to technological advances in thin film preparation and micro- and

¹ Corresponding author. Tel: +41-1-635-5776; fax: +41-1-635-5704; e-mail address: andreas.engel@physik.unizh.ch

nano-structuring methods during the last decade a whole range of novel superconducting devices exploiting various aspects of superconductivity have become technological feasible. Without being exhaustive examples are superconducting quantum interference devices [1,2], quantum computing [3] and quantum detectors [4]. For all of these devices to offer superior advantages compared to more conventional semiconducting devices low noise levels are one of several prerequisites. For macroscopic superconductors noise levels are usually very low because of the low operating temperatures and the formation of the superconducting energy gap $\Delta(T)$. However, as the size of the superconductor becomes comparable to the superconducting coherence length $\xi(T)$ in one or more dimensions fluctuation effects play an increasingly important role [5] in the overall performance of the device.

In this letter we will discuss fluctuation effects in superconducting nano-strips near the I - T phase transition. In previous studies fluctuations in superconductors with reduced dimensions have often been done in the limit of small applied currents [6]. In contrast, we consider fluctuations in the opposite limit of very high applied currents [7] close to the critical current $I_c(T)$, a situation that is often encountered in real applications, e.g. transition edge sensors [8]. We will consider two independent thermodynamically driven fluctuation types, which may lead to a localized and temporary transition to the normal state. One type are fluctuations of the number of superconducting charge carriers, i.e. Cooper pairs. Macroscopically this may be expressed as localized fluctuations in the critical current density. If the critical current density drops below the applied current density, the device will switch into a temporary resistive state. The other type of fluctuations are temporarily created bound vortex-antivortex pairs (VAPs). Under the acting Lorentz force due to the relatively high applied current density such bound vortices may unbind and move towards opposite edges of the strip [7]. Such vortex motion also leads to a resistive state. In both cases the fluctuations are detected as voltage transients developing between the meander ends.

2 Fluctuations in the Cooper-pair density

The number density of Cooper pairs in superconductors are subject to thermally activated fluctuations [9,10]. To evaluate their role in the voltage pulse rate in these superconducting strips we make use of a recently proposed refinement of the hotspot model in superconducting single photon detectors [11]. Suppose in a disc-like volume V with thickness equal to the film thickness $d < \xi(T)$ and radius a , $\xi(T) \leq 2a \leq w$, the number of Cooper pairs N_s decreases by δN_s , see also Fig. 1. Far from the fluctuation site and at temperatures well below the critical temperature T_c the current density is proportional to the velocity of the superconducting charge carriers [6], thus the current may

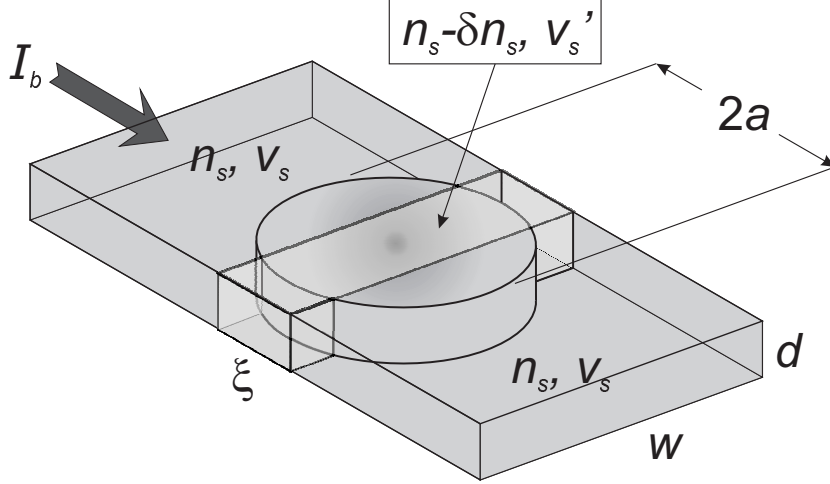


Fig. 1. Schematic drawing of the refined hotspot model. The grey shaded volume is a cloud with reduced Cooper-pair density $n_s - \delta n_s$. If the density is low enough such the mean pair velocity v'_s exceeds the critical velocity v_s^* in a cross-section with longitudinal extension ξ or larger, this cross-section switches into the normal conducting state.

be expressed as $I = n_s \bar{v}_s 2e wd$, with n_s the number of Cooper pairs per unit volume, \bar{v}_s the mean velocity of Cooper pairs and $2e$ their charge. Furthermore, we assume the current density to be homogeneous over the cross-section of the strip, because of the effective magnetic penetration length $\Lambda = \lambda_L(0)^2/d$ being much larger than the strip width and thickness. For a cross-section including the fluctuation volume the Cooper pair density is not homogeneous, anymore. However, one can easily show within Ginzburg-Landau (GL) theory that the supercurrent redistributes to keep the mean velocity of the superconducting charge carriers the same all over the cross-section as long as there is no magnetic flux linked to the fluctuation. Thus, the current is now given by $I = n_{s,\text{eff}} \bar{v}'_s 2e wd$, with $n_{s,\text{eff}} = n_s - \delta N_s/V$ and $\bar{v}'_s > \bar{v}_s$. The minimum critical fluctuation that drives the cross-section normal conducting is then given by the condition that \bar{v}'_s is equal to the critical velocity $\bar{v}_s^* \approx I_c/(n_s wd)$, I_c is the temperature dependent critical current. Using simple algebra this can be converted into the minimum number of Cooper pairs that need to be destroyed within the fluctuation volume

$$\delta N_s^* = \frac{\pi}{2} awd n_s \left(1 - \frac{I}{I_c}\right) \quad (1)$$

$$\approx \frac{\pi}{4} awd N_0 \Delta(I, T) \left(1 - \frac{I}{I_c}\right), \quad (2)$$

where in Eq. (2) we have used $n_s \approx (N_0/2)\Delta(I, T)$ for $T \ll T_c$, with N_0 the density of states at the Fermi energy and $\Delta(I, T)$ the superconducting energy gap or pairing potential.

The thermodynamic probability for such a fluctuation is given by $\exp[-\Delta F/k_{\text{B}}T]$ using the change in free energy ΔF associated with the fluctuation, k_{B} is the Boltzmann constant and T the temperature. For the change in free energy we used the minimum excitation energy $E_{\text{min}}(I, T)$ required to break one Cooper pair times the number of pairs broken:

$$\Delta F = \delta N_{\text{s}} E_{\text{min}}(I, T) \quad (3)$$

with the minimum excitation energy given as

$$\begin{aligned} E_{\text{min}}(I, T) &= \Delta(I, T) \left(1 - \frac{I}{I_{\text{c}}}\right) \\ &= \Delta_0 \left[1 - \left(\frac{T}{T_{\text{c}}}\right)^4\right]^{\frac{1}{2}} \left[1 - \alpha \left(\frac{I}{I_{\text{c}}}\right)^2\right] \left(1 - \frac{I}{I_{\text{c}}}\right). \end{aligned} \quad (4)$$

$\Delta_0 = 1.76k_{\text{B}}T_{\text{c}}$ is the BCS energy gap at zero temperature and the following term is a relatively simple analytical approximation to the BCS temperature dependence of the energy gap. An applied bias current further reduces the energy gap or pairing potential [12,13]. This contribution is generally of minor importance except at temperatures very close to T_{c} . We account for this contribution by the phenomenological parameter $\alpha = 0.03(1 - T/T_{\text{c}})^{-0.5}$. The dominant current-induced effect is a shift of the Fermi sphere in k -space which reduces the minimum excitation energy $E_{\text{min}} = \Delta - p_{\text{F}}v_{\text{s}}$, p_{F} is the momentum corresponding to the Fermi-energy [6]. Furthermore $\Delta \approx p_{\text{F}}v_{\text{s}}^*$ and using the above mentioned proportionality between the superconducting current and the speed of its carriers, we arrive at $E_{\text{min}} \propto (1 - I/I_{\text{c}})$.

Experimentally measured fluctuation rates are not only caused by minimum fluctuations needed to trigger a voltage pulse but by all fluctuations temporarily destroying more Cooper pairs than δN_{s}^* . Although larger fluctuations require more energy and are less frequent we take the integral over thermodynamic probabilities for fluctuations from the minimum number δN_{s}^* to the maximum number $n_{\text{s}} \pi a^2 d$. Furthermore, one has to take a second integral over the fluctuation volume given by the radius a . The minimum volume is given when all Cooper pairs within that volume have to be broken in order to cause a voltage pulse. It follows that the minimum radius is given by $a_{\text{min}} = (1 - I/I_{\text{c}})w/2$. If the bias current is close enough to I_{c} the minimum radius a_{min} becomes less than $\xi(T)$. Because variations on a scale smaller than $\xi(T)$ do not influence superconductivity an absolute minimum of $a_{\text{min}} = \xi(T)/2$ was set. As the upper limit of the fluctuation volume we defined the strip width w . Then, the overall thermodynamic probability for a dark count event caused by fluctuations of the number of Cooper pairs results as

$$P(I, T) = \int_{a_{\text{min}}}^{w/2} \int_{\delta N_{\text{s}}^*}^{n_{\text{s}} \pi a^2 d} \frac{Lw}{a^2} \exp\left(-\frac{\Delta F}{k_{\text{B}}T}\right) d\delta N_{\text{s}} da, \quad (5)$$

with

$$a_{\min} = \begin{cases} (1 - I/I_c) \frac{w}{2} & \text{for } (1 - I/I_c)w \geq \xi(T) \\ \frac{\xi(T)}{2} & \text{else.} \end{cases} \quad (6)$$

Fluctuations of different size a are weighted with the number of independent fluctuation sites Lw/a^2 . The fluctuation rate is obtained by multiplying the probability of Eq. (5) with an attempt rate $\Omega_{0,\text{cp}}$. In general, the attempt rate also depends on the the bias current, temperature and size of the fluctuations. Lacking a well-founded theoretical expression for the attempt rate we use it as an adjustable parameter to fit the experimental data.

3 Thermal unbinding of vortex-antivortex pairs

Another type of fluctuations is intimately linked to the Berezinskii–Kosterlitz–Thouless (BKT) transition in thin superconducting films [14,15,16]. Below the BCS transition temperature T_c in zero magnetic field excitations of the form of bound VAPs with no net flux may exist in two-dimensional films. Between the BKT transition temperature T_{BKT} and T_c bound pairs and thermally activated unbound vortices coexist. In the absence of pinning the unbound vortices lead to a finite resistance even below T_c . If a transport current is applied it exerts a Lorentz force which is opposite in direction for the two partners of a VAP. Thus no net force acts on a bound pair, but it leads to a preferred orientation of the pair and a reduction of the binding energy. Consequently, the combined action of the applied current and thermal activation may lead to pair-unbinding even below T_{BKT} . This current-assisted thermal unbinding (CATU) of VAPs may in turn be an important source of voltage pulses in the superconducting strips under investigation and is explored in more detail below.

Whether or not the above sketched BKT transition is an appropriate model for such NbN strips one should make sure that the strips fall within the two-dimensional (2D) limit and vortices can form in the strips. The NbN films have typical coherence lengths extrapolated to zero temperature of approximately 8 nm. With minimum strip widths of about 80 nm, $\xi(T) < w$ for all temperatures except very close to T_c . Likharev [17] gives a criterium for the minimum strip width for the existence of vortices: $w \geq 4.4\xi(T)$. This more stringent criterium is also fulfilled for the temperatures of interest, i.e. for which fluctuation rates were measured. These theoretical considerations are backed by an analysis of the resistive transition of a sample shown in Fig. 2 together with appropriate least-square fits for the different temperature intervals (solid lines). The resistance data was collected with a standard 4-wire setup and the sample immersed in liquid or gaseous helium at temperatures below and above 4.2 K, respectively. The rounding of the transition above T_c is assumed to be due to fluctuation conductivity of the Aslamazov-Larkin type [18] in a

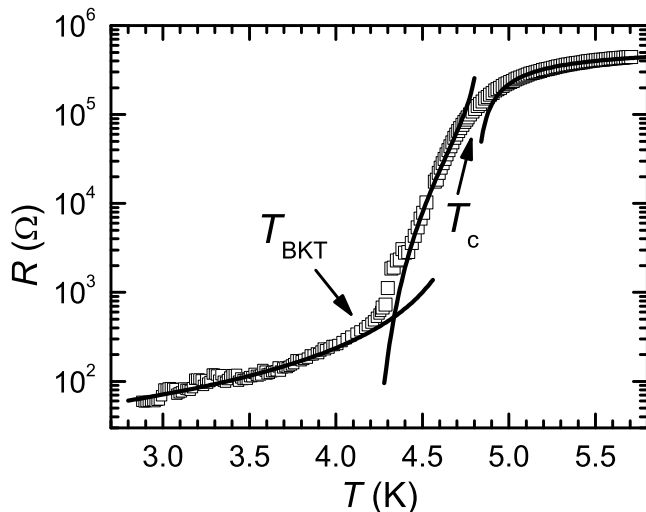


Fig. 2. Resistive transition of a 5 nm thick NbN meander. The solid lines are least-square fits for the various temperature intervals as described in the text. The BCS and BKT transition temperatures are indicated by arrows.

dirty superconducting 2D-film with a high sheet resistance

$$\sigma_{2D} = \frac{1}{16} \frac{e^2}{\hbar d} \frac{T_c}{T - T_c}, \quad (7)$$

with e the elementary charge and $\hbar = h/2\pi$ Planck's constant. Fitting of the resistance data in the relevant temperature region using Eq. (7) allowed to extract the transition temperature $T_c = 4.81$ K and the normal state sheet resistance $R_s = 1.4$ k Ω . Below T_c the resistance is dominated by thermally unbound VAPs and the BKT theory gives its temperature dependence as [19]

$$R \propto \exp \left[-2 \left(b \frac{T_c - T}{T - T_{\text{BKT}}} \right)^{1/2} \right], \quad (8)$$

with b a parameter from the theory. For an infinite 2D-film the resistance should vanish below the BKT transition temperature, which turned out to be $T_{\text{BKT}} = 4.14$ K for this meander. In a finite sample, however, free vortices are present even below T_{BKT} and Mooij [19] gives the following relation for the sheet resistance:

$$\frac{R_s}{R_N} = 2\pi y(l_w) \exp(-2l_w), \quad (9)$$

with a length scale $l_w = \ln[w/\xi(T)]$ and $y(l_w)$ is the pair excitation probability containing the temperature dependence. Following some of the simplifications

in Ref. [19] Eq. (9) can be expressed as

$$R_s \approx 2\pi R_N \left(\frac{\xi(T)}{w} \right)^\eta \quad (10)$$

and the exponent η is of the order of 1. Using the simple GL-relation $\xi(T) = \xi_0(1 - T/T_c)^{-1/2}$ a best fit was obtained for $\eta = 3$. The temperature independent prefactor of the least-square fit equaling 16.4 also compares very well with the theoretical value $2\pi R_N(\xi_0/w)^3 \approx 12$. The above sketched analysis gives a self-consistent description of the resistive transition in terms of a BKT-transition in a finite 2D superconducting film, thus we conclude that VAPs do exist in these structures².

Coming back to the question of how VAPs might influence the count rates of random voltage pulses, we note that the count rates were measured at temperatures well below T_{BKT} . Free vortices present due to finite size effects will be neglected. Their average number was estimated from the areal density based on the resistance measurement and turned out to be much smaller than the number of unbound vortices due to the high bias current. As mentioned above VAPs will orientate themselves with respect to the bias current near the orientation with minimum binding energy

$$U_b = 2\mu_c + \frac{A(T)}{\varepsilon(l_j)}(l_j - 1). \quad (11)$$

Here $l_j = \ln(2.6j_c/j)$ is a current scale, j_c the critical current density and j the applied current density, and $\varepsilon(l_j)$ is a renormalization factor close to unity. The temperature dependent energy scale $A(T) = (\pi^2\hbar/2e^2R_s)\Delta(T)\tanh[\Delta(T)/k_B T]$ has to be calculated from device parameters, where $\Delta(T)$ is the superconducting energy gap at zero current, and μ_c is the core energy of one vortex. The unbinding process can be seen as thermal excitation requiring the energy U_b . After the thermal unbinding vortex and antivortex are accelerated due Lorentz forces and move in opposite directions towards the strip edges where they annihilate. Assuming free flux-flow according to the Bardeen-Stephen model the voltage signal developing between the strip ends is comparable in height to the voltage pulses caused by the thermodynamic fluctuations of the order parameter described above. Also, the pulse duration is expected to be of the same order of about 1 ns or less, so that these two fluctuation modes are not easily discriminated.

For a thermally activated unbinding process the count rate should be proportional to $\exp(-U_b/k_B T)$. The core energy μ_c in Eq. (11) may be a non-

² In this context open questions remain with regard to the Likharev criterium, which prohibits vortices for a non-negligible temperature range between T_c and T_{BKT} , and the role of edge barriers in narrow superconducting strips expelling vortices [20].

negligible contribution to U_b . Generally, it is assumed to be approximately proportional to the energy scale $A(T)$, i.e. $\mu_c \approx A(T)/\gamma$, $\gamma = \text{const}$. Then the count rate may be expressed as

$$\Gamma_{\text{BKT}}(I, T) = C \left(\frac{I}{2.6I_c} \right)^{\frac{1}{\varepsilon(l_j)} \frac{A(T)}{k_B T}}, \quad (12)$$

with $C = \Omega_{0,\text{BKT}} \exp[\beta A(T)/k_B T]$, $\Omega_{0,\text{BKT}}$ the attempt rate and $\beta = [\gamma - 2\varepsilon(l_j)]/[\gamma\varepsilon(l_j)]$ a parameter of order unity.

4 Experimental details

The samples were made from a $d = 5$ nm thick NbN film on a sapphire substrate. The film was prepared by dc magnetron sputtering in an Ar/N₂ gas mixture. The N₂ concentration was reduced with respect to the optimal concentration for a stoichiometric composition. Together with high sputtering rates (1.2 nm/s) and the substrate not being heated this resulted in films with a reduced N-content and a high degree of disorder. Consequently, the films had critical temperatures T_c approximately 5 to 6 K, only about one third of the critical temperature in bulk NbN. Using a combination of electron-beam and photolithography the films were structured by reactive ion etching into a meander covering an area of roughly $4 \times 4 \mu\text{m}^2$. The device used for the fluctuation measurements had a strip width $w = 84$ nm and a total length $L = 36 \mu\text{m}$. Partial damage due to the etching process caused nonsuperconducting areas at the strip edges inferred from independent measurements to be about 4 nm thick. Also, thin layers (0.4 nm) at the top and bottom of the film are assumed to be normal conducting. Proximity effects associated with these normal conducting areas lead to a further reduction of the critical temperature to the above mentioned 4.81 K for the present sample. A zero temperature coherence length $\xi_0 = 8.5$ nm was deduced from magnetoconductivity measurements and the London penetration depth $\lambda_L(0) \gtrsim 300$ nm was estimated [21,22]. The electronic density of states at the Fermi energy $N_0 = 2.2 \cdot 10^{24} \text{ m}^{-3} \text{ K}^{-1}$ was deduced from Einstein's relation $N_0 = 1/(e^2 \rho D)$, with the diffusion coefficient $D = 0.35 \text{ cm}^2 \text{ s}^{-1}$ determined from $B_{c2}(T)$ near T_c .

The device was thermally anchored to the cold plate of a ⁴He bath cryostat. The temperature was controlled via the vapor pressure of the helium bath. The bias current was supplied by a low-noise custom-made biasbox in constant-voltage mode. An additional low-pass filter at the entrance to the cryostat and a voltage divider inside, close to the device, allowed to adjust the bias current reliably, even very close to $I_c(T)$. Fluctuation events were registered as hf voltage signals which were passed on to a microwave amplifier chain with an

effective band pass from 0.1 to 1.6 GHz and a total gain ≈ 50 dB. To reduce parasitic noise the first stage was a cryogenic amplifier with a very low noise temperature of 6 K. Amplified voltage pulses were fed into either a digital 250 MHz bandwidth/1 GHz sampling rate oscilloscope or a 200 MHz bandwidth voltage-level counter. NbN meanders like to one used in this investigation can be utilized as single photon detectors with a quantum efficiency of $\approx 10\%$ in the visible and nearinfrared spectral range [23,24]. Absorbed photons produce voltage signals very similar to the pulses caused by those fluctuations considered in this paper, in fact, they may be the limiting factor of the sensitivity of such detectors. Intrinsic to these detectors is a cutoff wavelength such that only photons with shorter wavelengths are detected. Assuming blackbody radiation from the surfaces facing the meander ($T \approx 4$ and 77 K, respectively), the number of detectable photons crossing the meander area is estimated to less than 10 photons/s. Considering a maximum detection efficiency of a few percent and the fact that the cut-off wavelength decreases with decreasing bias current [11,24], the background photons can be safely neglected for all measurements.

5 Results and discussion

Voltage pulse rates were recorded as a function of the applied bias current at fixed temperatures. In Fig. 3 data for three different temperatures $T = 3.6, 3.3,$ and 2.85 K are shown. At the highest temperature (squares in Fig. 3) the data nearly follow an exponential dependence. However, as the temperature is reduced, the data deviate more and more from such a simple relation and open up the question as to the origin of such a temperature and current dependence. One might think of various mechanisms being able to produce voltage pulses similar to those observed in our experiments, though some of which can be ruled out. Photons of sufficient energy are certainly capable of causing such signals. However, estimates as outlined in the previous section quickly show that background radiation is many orders of magnitude too low to give any significant contribution to the observed count rates. Thermal [25,26] and quantum phase slips [27,28] are also expected to play a minor role, since the strip width is still considerably larger than the coherence length. Although great efforts have been made to reduce noise superimposed on the bias current contributions from current noise cannot be ruled out so easily. Especially for bias currents extremely close to I_c current noise will add to the dark count rates as well as temperature fluctuations and associated fluctuations in I_c . However, the observed temperature dependence is not easily explained by such extrinsic noise sources. Therefore, we tried to analyze the experimental data in light of the fluctuation modes discussed in the previous Sec. 2 and 3.

The solid lines in Fig. 3 are least-square fits of Eq. 12 to the experimental data.

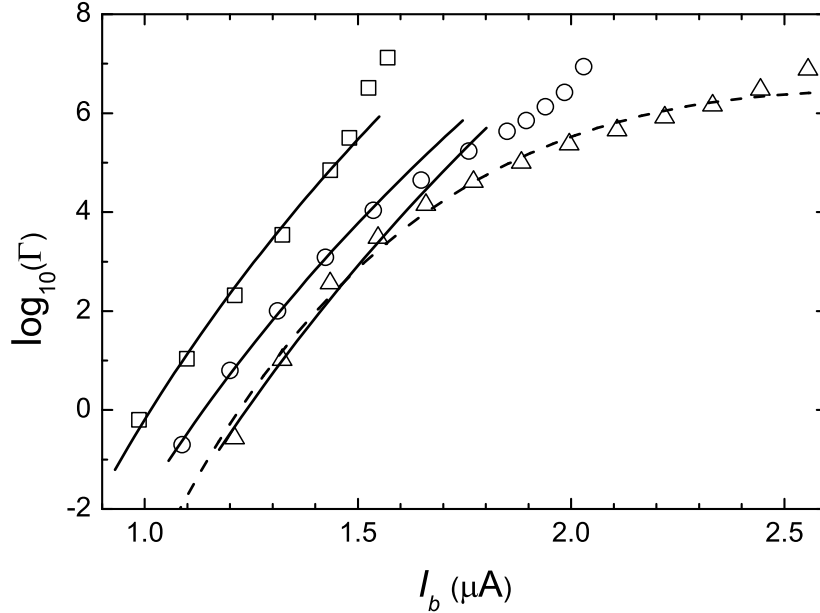


Fig. 3. Dark count rates vs bias current for temperatures $T = 3.6, 3.3$ and 2.85 K from left to right. The solid lines are least-square fits according to Eq. 12. The dashed line includes a phenomenological currentdependence of $\varepsilon(l_j)$.

The energy scale $A(T)$ was calculated independently for each temperature and $\varepsilon(l_j)$ and C were taken as current independent fitting parameters. For the highest temperature of $T = 3.6$ K this results in a satisfactory fit with parameters $\varepsilon(l_j) = 0.67$ and an attempt rate $\Omega_{0,\text{BKT}} = 9 \cdot 10^9 \text{ s}^{-1}$, assuming $\beta \approx 1$. At lower temperatures this approach works at low currents, only, but still with comparable parameters $\varepsilon(l_j) = 0.85$, $\Omega_{0,\text{BKT}} = 2.5 \cdot 10^9 \text{ s}^{-1}$ and $\varepsilon(l_j) = 1.0$, $\Omega_{0,\text{BKT}} = 3.8 \cdot 10^{10} \text{ s}^{-1}$ at $T = 3.3$ and 2.85 K, respectively. So far, the current dependence of $\varepsilon(l_j)$, indicated by the subscript j , has been neglected. We have made this simplification partly because the BKT-theory makes only vague statements on its current dependence. Yet, if one allows for a current dependence of $\varepsilon(l_j)$, albeit phenomenologically, the fit at low temperatures can be substantially improved. The dashed curve in Fig. 3 was obtained for ε decreasing from 1.0 at low currents to about 0.75 very close to I_c . Even though the resulting curve describes the data very well, we would like to stress that it is not based on a sound theoretical model. Alternatively, one might think of mechanisms that set a limit to the count rate caused by the unbinding process in this BKT-model, which would also manifest itself in a kink similar to that observed.

As the bias current approaches the critical current the count rates for all temperatures exhibit an upturn contradictory to expectations based on the unbinding of VAPs. This is when fluctuations of the Cooper pair density may come into play. Count rates based on Eq. 5 have to be calculated numerically and fitted to the experimental data by adjusting the attempt rate $\Omega_{0,\text{cp}}$. In

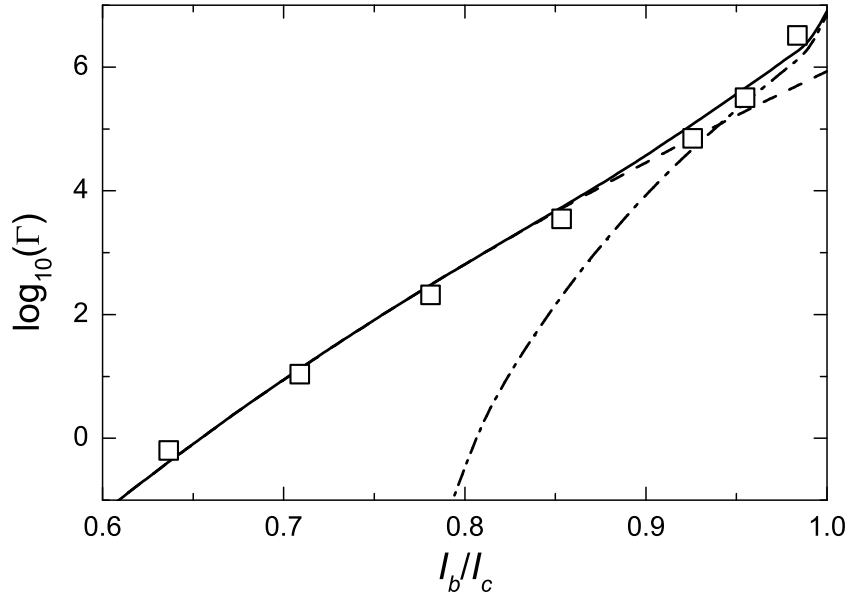


Fig. 4. Dark count rate vs reduced bias current at $T = 3.6$ K. The dashed line is the least-square fit of Fig. 3 and the dash-dotted curve the dark count rate obtained for fluctuations of the superconducting order parameter. The solid curve is the sum of these two contributions.

doing so, it soon becomes apparent that these fluctuations may only be of importance for bias currents very close to the critical current, exceeding $\approx 0.9I_c$. In Fig. 4 the count rate at 3.6 K is shown versus the reduced current I/I_c . The dashed curve is the best fit according to VAP unbinding model and the dash-dotted curve is the contribution from the Cooper pair fluctuations using an attempt rate $\Omega_{0,cp} = 1.6 \cdot 10^8 \text{ s}^{-1}$. The sum of both fluctuation modes extends the excellent agreement between experiment and theoretical description up to the highest applied currents $I/I_c \approx 0.98$. It has to be noted however, that for bias currents sufficiently close to I_c current noise will certainly add to the observed dark count rate and the observed upturn may, at least in part, be caused by this noise contribution.

6 Conclusions

In summary, we have described current and temperature dependent fluctuation effects in superconducting nanostructures, which were detected as voltage pulses in long meander lines. Current-assisted thermal unbinding of vortex-antivortex pairs turned out to be the the most likely source of count rates over most of the current range. For high bias currents extremely close to the critical current fluctuations in the number density of Cooper pairs need to be considered, as well. For the application of single-photon counters and other

low-dimensional superconducting devices the detailed knowledge of the origins and control of superconducting fluctuations will be an important issue to choose the optimum operating conditions and additional investigations will be necessary. We are very grateful to D. Golubev for stimulating discussions.

References

- [1] D. Koelle, R. Kleiner, F. Ludwig, E. Dantsker, C. J., High-transition-temperature superconducting quantum interference devices, *Rev. Mod. Phys.* 71 (1999) 631.
- [2] J. Oppenländer, C. Häussler, T. Träuble, N. Schopohl, Superconducting multiple loop quantum interferometers, *IEEE Trans. Appl. Supercond.* 11 (2001) 1271.
- [3] Y. Nakamura, Y. A. Pashkin, J. S. Tsai, Coherent control of macroscopic quantum states in a single-cooper-pair box, *Nature* 398 (1999) 786.
- [4] A. Peacock, P. Verhoeve, N. Rando, A. v. Dordrecht, B. G. Taylor, C. Erd, M. A. C. Perryman, R. Venn, J. Howlett, D. J. Goldie, M. Lumley, J. Wallis, Single optical photon detection with a superconducting tunnel junction, *Nature* 381 (1996) 135.
- [5] W. J. Skocpol, M. Tinkham, Fluctuations near superconducting phase transitions, *Rep. Prog. Phys.* 38 (1975) 1049.
- [6] M. Tinkham, *Introduction to Superconductivity*, 2nd Edition, McGraw-Hill, Inc., New York, 1996.
- [7] C. M. Knoedler, R. F. Voss, Voltage noise measurement of the vortex mean free path in superconducting granular tin films, *Phys. Rev. B* 26 (1982) 449.
- [8] A. T. Lee, P. L. Richards, S. W. Nam, B. Cabrera, K. D. Irwin, A superconducting bolometer with strong electrothermal feedback, *Appl. Phys. Lett.* 69 (1996) 1801.
- [9] C. M. Wilson, L. Frunzio, D. E. Prober, Time-resolved measurements of thermodynamic fluctuations of the particle number in a nondegenerate Fermi gas, *Phys. Rev. Lett.* 87 (2001) 067004.
- [10] C. M. Wilson, D. E. Prober, Quasiparticle number fluctuations in superconductors, *Phys. Rev. B* 69 (2004) 094524.
- [11] A. Semenov, A. Engel, H.-W. Hübers, K. Il'in, M. Siegel, Probability of the resistive state formation caused by absorption of a single-photon in current-carrying superconducting nano-strips, submitted to *Eur. Phys. J.* Preprint available at cond-mat/0410633.
- [12] J. L. Levine, Dependence of superconducting energy gap on transport current by the method of electron tunneling, *Phys. Rev. Lett.* 15 (1965) 154.

- [13] A. Anthore, H. Pothier, D. Esteve, Density of states in a superconductor carrying a supercurrent, *Phys. Rev. Lett.* 90 (2003) 127001.
- [14] Z. L. Berezinskii, *Zh. Eksp. Teor. Fiz.* 59 (1970) 907.
- [15] Z. L. Berezinskii, *Zh. Eksp. Teor. Fiz.* 61 (1971) 1144.
- [16] J. M. Kosterlitz, D. J. Thouless, Ordering, metastability and phase transitions in two-dimensional systems, *J. Phys. C* 6 (1973) 1181.
- [17] K. K. Likharev, Superconducting weak links, *Rev. Mod. Phys.* 51 (1979) 101.
- [18] L. G. Aslamazov, A. I. Larkin, The influence of fluctuation pairing of electrons on the conductivity of normal metal, *Phys. Lett.* 26A (1968) 238.
- [19] J. E. Mooij, Two-dimensional transition in superconducting films and junction arrays, in: A. M. Goldman, S. A. Wolf (Eds.), *Percolation, Localization, and Superconductivity*, Plenum Press New York, 1984, p. 325.
- [20] G. Stan, S. B. Field, J. M. Martinis, Critical field for complete vortex expulsion from narrow superconducting strips, *Phys. Rev. Lett.* 92 (2004) 097003.
- [21] D. E. Oates, A. C. Anderson, C. C. Chin, J. S. Derov, G. Dresselhaus, M. S. Dresselhaus, Surface-impedance measurements of superconducting NbN films, *Phys. Rev. B* 43 (1991) 7655.
- [22] S. Kubo, M. Asahi, M. Hikita, M. Igarashi, Magnetic penetration depths in superconducting NbN films prepared by reactive dc magnetron sputtering, *Appl. Phys. Lett.* 44 (1984) 258.
- [23] A. Engel, A. Semenov, H.-W. Hübers, K. Ilin, M. Siegel, Dark counts of a superconducting single-photon detector, *Nucl. Instr. and Meth. A* 520 (2004) 32.
- [24] A. Engel, A. Semenov, H.-W. Hübers, K. Il'in, M. Siegel, Superconducting single-photon detector for the visible and infrared spectral range, *J. Mod. Optics* 51 (2004) 1459.
- [25] J. S. Langer, V. Ambegaokar, Intrinsic resistive transition in narrow superconducting channels, *Phys. Rev.* 164 (1967) 498.
- [26] D. E. McCumber, B. I. Halperin, Time scale of intrinsic resistive fluctuations in thin superconducting wires, *Phys. Rev. B* 1 (1970) 1054.
- [27] A. D. Zaikin, D. S. Golubev, A. van Otterlo, G. T. Zimányi, Quantum phase slips and transport in ultrathin superconducting wires, *Phys. Rev. Lett.* 78 (1997) 1552.
- [28] D. S. Golubev, A. D. Zaikin, Quantum tunneling of the order parameter in superconducting nanowires, *Phys. Rev. B* 64 (2001) 014504.